JOURNAL OF MATERIALS SCIENCE 20 (1985) 3750–3762

On fracture initiation in a material with an ellipsoidal inclusion

MANABU TANAKA, HIROSHI IIZUKA
Department of Mechanical Engineering for Production, Mining College of Akita University, Akita 010, Japan

Fracture initiation at the interface of an inclusion in a metallic material both at room and elevated temperatures, using the equivalent inclusion method, is discussed theoretically. It is shown that the critical strain for fracture initiation at the interface of the inclusion is strongly affected by shape, size, orientation and rigidity of the inclusion, and by the presence of external stress. Dynamic recovery by diffusion of atoms has a large effect on the decohesion at the inclusion–matrix interface in the high-temperature range. Fracture initiation of a brittle material strengthened with strong fibres is also discussed.

1. Introduction

Most non-metallic inclusions contained in metallic materials are usually very hard to deform and often become the origin of fracture in those materials.

Mori *et al.* [1, 2] discussed fracture initiation at the interface of a spherical, fibre or disc inclusion during tensile deformation of the material, using the equivalent inclusion method [3]. However, little work has been performed on fracture initiation at the interface of an ellipsoidal inclusion with arbitrary aspect ratio [4] or on the decohesion at the interface of the inclusion in the high-temperature range where recovery due to diffusion of atoms occurs [5].

In this study, a theoretical discussion was undertaken on the effects of several factors, including shape, size, orientation and rigidity of an inclusion, on fracture initiation at the inclusion–matrix interface both at room and elevated temperatures, using the equivalent inclusion method and the results of a previous study [6].

In a ceramic strengthened with strong fibres, a large tensile stress (internal stress) occurs in the fibres in the matrix, causing either decohesion at the interface of fibres or fracture of the matrix as a result of phase transformation or difference in thermal expansion between fibres and matrix [7]. Fracture initiation in a brittle material is also discussed.

2. Stress and energy conditions for fracture initiation

The deformation of a metallic material with an ellipsoidal inclusion ($(x_1^2 + x_2^2)/a^2 + x_3^2/c^2 = 1$; volume of inclusion, $V = \frac{4}{3}\pi a^2 c$; aspect ratio, $x = c/a$) is considered. The elastic constants of the inclusion, C^*_{ijkl}, are different from those of the matrix, C_{ijkl}. Fig. 1 shows an ellipsoidal inclusion in the matrix. It is considered that a uniform plastic deformation ($e^*_{33} = \varepsilon^*$, $e^*_{11} = e^*_{22} = -\varepsilon^*/2$ in (x_1, x_2, x_3) coordinates) occurs only in the matrix due to an applied tensile stress σ^A_{33}. The stress state in this case is identical to that when the eigenstrains, $\varepsilon^*_{33} = -2\varepsilon^*_{11} = -2\varepsilon^*_{22} = -\varepsilon^*$, occur only in the inclusion under an applied stress, σ^A_{33} [3]. The total stress in an inclusion, σ^I_{ij}, is the sum of the internal stress with the eigenstrains $(\sigma^I_{ij})_{int}$ (plastic deformation effect) plus the disturbed applied stress field due to rigidity effect, $(\sigma^I_{ij})_{inh}$. The stress condition for fracture initiation at the interface of the inclusion is satisfied [1] when

$$\sigma^I_{33} = (\sigma^I_{33})_{int} + (\sigma^I_{33})_{inh} \geqslant E^*/10 \text{ or } E/10 \quad (1)$$

where $E^* = 2\mu^*(1 + \nu^*)$ and $E = 2\mu(1 + \nu)$

0022–2461/85 $03.00 + .12

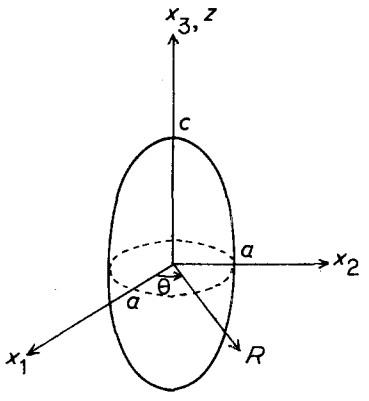

Figure 1 An ellipsoidal inclusion and Cartesian coordinate system.

are Young's modulus of the inclusion and that of the matrix, respectively. The critical strain for stress condition, ε_c^{*s}, can be calculated from Equation 1. The stress components are obtained by the equivalent inclusion method [1–3, 7]:

$$(\sigma_{ij}^{I})_{int} = C_{ijkl}(e_{kl}^{c} - e_{kl}^{T}) = C_{ijkl}^{*}(e_{kl}^{c} - \varepsilon_{kl}^{*}) \quad (2)$$

$$(\sigma_{ij}^{I})_{inh} = C_{ijkl}(e_{kl}^{c'} + e_{kl}^{A} - e_{kl}^{T'}) = C_{ijkl}^{*}(e_{kl}^{c'} + e_{kl}^{A}) \quad (3)$$

where $e_{kl}^{c} = S_{klmn}e_{mn}^{T}$, $e_{kl}^{c'} = S_{klmn}e_{mn}^{T'}$ and $e_{kl}^{A} = C_{klij}^{-1}\sigma_{ij}^{A}$. Here S_{klmn} is the Eshelby tensor [3], and e_{mn}^{T} and $e_{mn}^{T'}$ are functions of ε_{kl}^{*} and e_{kl}^{A}, respectively. The internal stresses immediately after fracture initiation can also be calculated by Equations 2 and 3, provided that the elastic constants of the inclusion after decohesion are given as follows [1]:

$$\begin{aligned} C_{1111}^{*} &= C_{2222}^{*} = E^{*}/(1 - \nu^{*2}) \\ C_{1122}^{*} &= C_{2211}^{*} = \nu^{*}E^{*}/(1 - \nu^{*2}) \\ C_{3333}^{*} &= C_{1133}^{*} = C_{3311}^{*} \\ &= C_{2233}^{*} = C_{3322}^{*} = 0 \end{aligned} \quad (4)$$

The Gibbs free energy of the material with an inclusion before and after decohesion, G_1 and G_2 respectively [1], are given by

$$G_1 = \tfrac{1}{2}A_1\mu\varepsilon^{*2}V + B_1\sigma_{33}^{A}\varepsilon^{*}V + \bar{D}_1\sigma_{33}^{A2}/2\mu + S\gamma_{I-M} \quad (5)$$

$$G_2 = \tfrac{1}{2}A_2\mu\varepsilon^{*2}V + B_2\sigma_{33}^{A}\varepsilon^{*}V + \bar{D}_2\sigma_{33}^{A2}/2\mu + S(\gamma_I + \gamma_M) \quad (6)$$

Here the first and second terms are the elastic strain energy and the interaction energy between internal stress field and external stress, respectively, and the third term is the energy term associated with the rigidity effect. A, B and $\bar{D}$ are shape factors, given in the Appendix. Subscripts 1 and 2 in these equations denote quantities before and after the initiation of fracture, respectively. S is the surface area of an inclusion. γ_I, γ_M and γ_{I-M} are the surface energies of the inclusion and of the matrix and the interface energy per unit area, respectively. It was assumed that Poisson's ratio of the inclusion, ν^{*}, is the same as that of the matrix, ν, and that

$$\gamma_M = Ea_0/10 = \mu(1 + \nu)a_0/5$$
$$\gamma_I = \mu^{*}(1 + \nu)a_0/5$$

where $a_0 = 3.61 \times 10^{-10}$ m is the lattice constant of the inclusion and the matrix, and $\gamma_{I-M} = |\gamma_M - \gamma_I|$ [1].

The energy condition for fracture initiation is satisfied if $G_1 > G_2$ [1]. The critical strain ε_c^{*e} for $G_1 = G_2$ is given by

$$\varepsilon_c^{*e} = -\frac{B_1 - B_2}{A_1 - A_2}\frac{\sigma_{33}^{A}}{\mu} + \left(\frac{4(1 + \nu)a_0S}{5(A_1 - A_2)V}\right)^{1/2} \quad \text{for } \mu^{*} > \mu \quad (7)$$

$$\varepsilon_c^{*e} = -\frac{B_1 - B_2}{A_1 - A_2}\frac{\sigma_{33}^{A}}{\mu} + \left(\frac{4m(1 + \nu)a_0S}{5(A_1 - A_2)V}\right)^{1/2} \quad \text{for } \mu^{*} \leqslant \mu \quad (8)$$

where $m = \mu^{*}/\mu$. The energy condition is satisfied when $\varepsilon^{*} > \varepsilon_c^{*e}$. Here σ_{33}^{A} should be replaced by σ_{11}^{A} and the permutation of indices should be applied to the quantities in Equations 1 and 4 to 8 when the external stress is σ_{11}^{A} and the eigenstrains are $\varepsilon_{11}^{*} = -2\varepsilon_{22}^{*} = -2\varepsilon_{33}^{*} = -\varepsilon^{*}$.

Figs. 2 and 3 show the result of calculation by Equations 7 and 8. The volume of an inclusion is kept constant ($V = \frac{4}{3}\pi a^2c = \frac{4}{3}\pi a^{*3}$ = constant) in this calculation. Both ε_c^{*s} and ε_c^{*e} are strongly affected by aspect ratio ($x = c/a$), orientation and rigidity of the inclusion. Both the energy and stress conditions are satisfied when $\varepsilon^{*} > \varepsilon_c^{*e}$ and $\varepsilon^{*} \geqslant \varepsilon_c^{*s}$. ε_c^{*s} is independent of particle size (full curves), but ε_c^{*e} increases with decrease of particle size (broken curves). The effect of applied stress on ε_c^{*e} and ε_c^{*s} is also dependent on x, m and orientation of the inclusion.

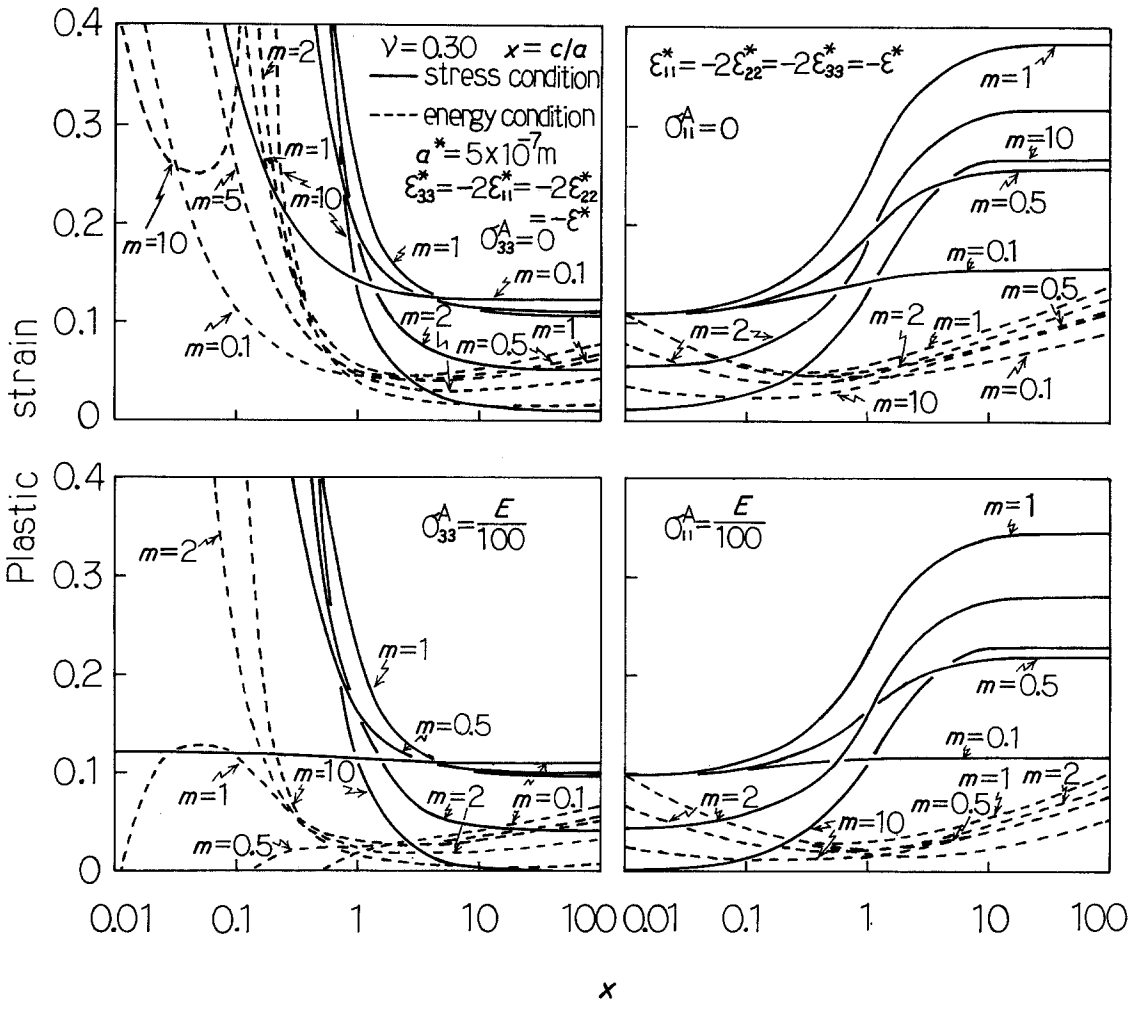

Figure 2 Relation between aspect ratio (x) and the critical strain for fracture initiation at the interface of an inclusion.

3. Effect of dynamic recovery on fracture initiation at the interface

The recovery effect due to diffusion of atoms on fracture initiation at the interface of the inclusion should be taken into account at elevated temperatures. The relationship between the eigenstrain ε^* and the observed plastic strain during the deformation, ε, under a constant (plastic) strain rate, $\dot{\varepsilon}$, is given by [6]

$$\varepsilon^* = (\dot{\varepsilon}/C)[1 - \exp(-C\varepsilon/\dot{\varepsilon})] \quad (9)$$

The value of C is dependent on temperature, on shape and size of the inclusion and on dynamic recovery process [6], as shown in Table I. Using Equation 9, the critical strain for the stress

TABLE I Relation between C and aspect ratio x

	$\varepsilon^*_{33} = -2\varepsilon^*_{11} = -2\varepsilon^*_{22} = -\varepsilon^*$			$\varepsilon^*_{11} = -2\varepsilon^*_{22} = -2\varepsilon^*_{33} = -\varepsilon^*$
	$x < 1$	$x = 1$	$x > 1$	$x \lesssim 1$
$C\Big/\left(\frac{9A_1\mu\Omega D_v}{4kT}\right)$	$\frac{1}{a^{*2}x^{1/3}}$	$\frac{1}{a^{*2}}$	$\frac{1}{a^{*2}x^{4/3}}$	$\frac{x^{2/3}}{a^{*2}}$
$C\Big/\left(\frac{9A_1\mu\Omega D_{GB}\delta}{2kT}\right)$	$\frac{1}{a^{*3}}$	$\frac{1}{a^{*3}}$	$\frac{1}{a^{*3}x}$	$\frac{(1+x)}{2a^{*3}}$

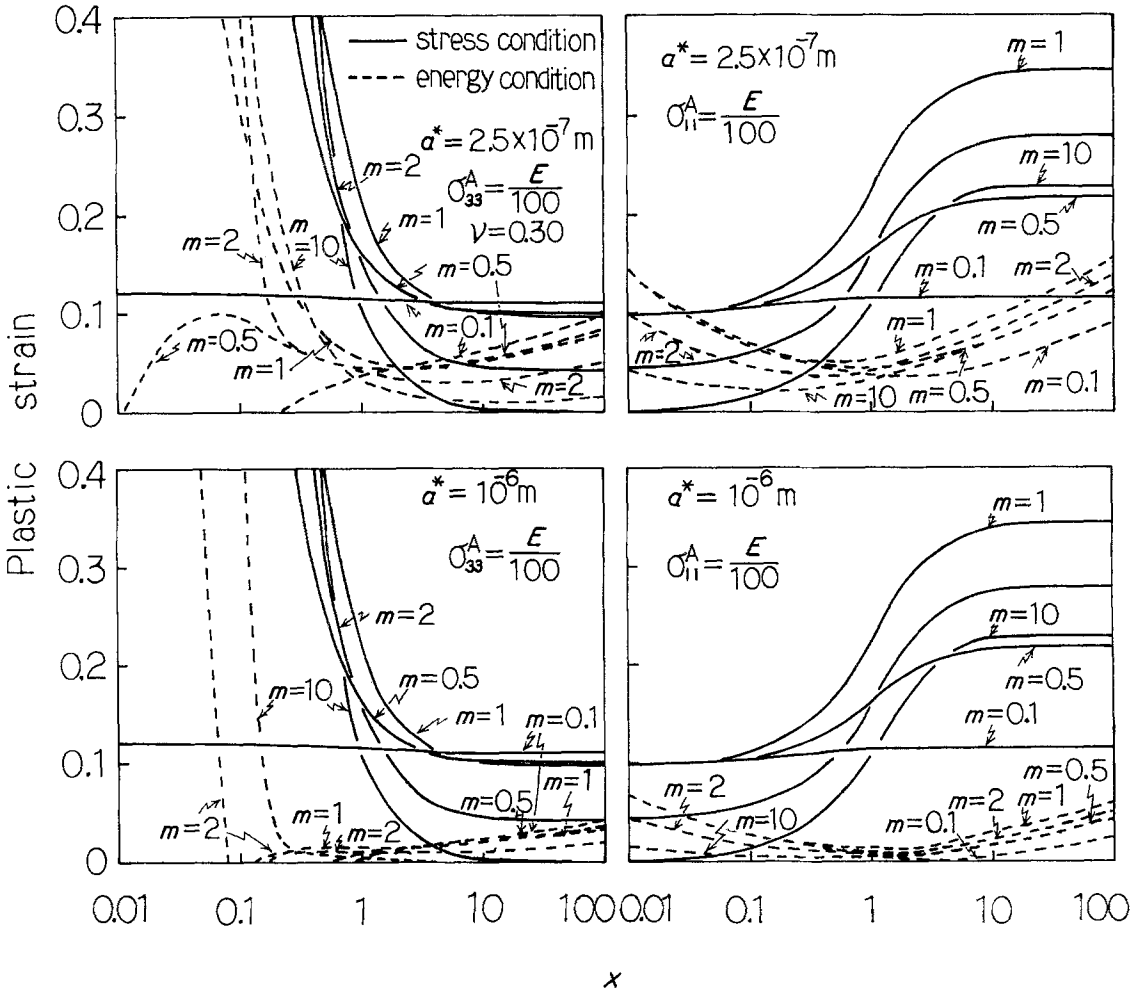

Figure 3 Effect of particle size on the critical strain for fracture initiation at the interface of an inclusion.

condition, ε_c^s, and that for the energy condition, ε_c^e, in this case are respectively given by

$$\varepsilon_c^s = -(\dot{\varepsilon}/C)\ln(1 - C\varepsilon_c^{*s}/\dot{\varepsilon}) \quad (10)$$

$$\varepsilon_c^e = -(\dot{\varepsilon}/C)\ln(1 - C\varepsilon_c^{*e}/\dot{\varepsilon}) \quad (11)$$

Figs. 4 and 5 show the relation between ε_c^e, ε_c^s and x where dynamic recovery due to volume diffusion or grain boundary diffusion is taken into account. The numerical values used in this calculation are $D_v = 8.30 \times 10^{-18}\,m^2\,sec^{-1}$ (1073 K) [6], $D_{GB} = 1.15 \times 10^{-14}\,m^2\,sec^{-1}$ (873 K) [8], grain boundary thickness $\delta \simeq 2b = 5.10 \times 10^{-10}$ m, molar volume of the matrix $\Omega = 7.10 \times 10^{-6}\,m^3$, $\mu = 5.83 \times 10^4$ MPa [6], $\nu = 0.30$ and $\dot{\varepsilon} = 1.33 \times 10^{-4}\,sec^{-1}$. The volume of an inclusion is also kept constant in the calculation. Strains ε_c^s and ε_c^e are both dependent on size, shape and orientation of the inclusion and on the recovery process.

4. Stresses at the interface of an inclusion

Stress components just outside an inclusion can also be obtained as a function of Eshelby tensor. The stress components arising from the rigidity effect have been calculated by other investigators [9, 10]. The stress components responsible for fracture initiation are shown as follows.

4.1. Inclusion with eigenstrains, $\varepsilon^*_{33} = -2\varepsilon^*_{11} = -2\varepsilon^*_{22} = -\varepsilon^*$, under an applied stress, σ^A_{33}

At equator points of an inclusion ($(a, 0, 0)$ and so on), the stress component due to plastic deformation effect, $(\sigma^M_{33})_{int}$, and that arising from

the rigidity effect, $(\sigma_{33}^{M})_{inh}$, are given by

$$
\begin{aligned}
(\sigma_{33}^{M})_{int} &= \frac{2\mu}{1-2\nu}\left[\left(2\nu(S_{1111}+S_{1122})+2(1-\nu)S_{3311}-\frac{\nu}{1-\nu}\right)e_{11}^{T}\right.\\
&\quad\left.+\left(2\nu S_{1133}+(1-\nu)S_{3333}-\frac{\nu^2}{1-\nu}\right)e_{33}^{T}\right]\\
(\sigma_{33}^{M})_{inh} &= \frac{2\mu}{1-2\nu}\left[\left(2\nu(S_{1111}+S_{1122})+2(1-\nu)S_{3311}-\frac{\nu}{1-\nu}\right)e_{11}^{T'}\right.\\
&\quad\left.+\left(2\nu S_{1133}+(1-\nu)S_{3333}-\frac{\nu^2}{1-\nu}\right)e_{33}^{T'}\right]+\sigma_{33}^{A}
\end{aligned}
\tag{12}
$$

The stress components at polar point (0, 0, c) are given by

$$
\begin{aligned}
(\sigma_{33}^{M})_{int} &= (\sigma_{33}^{I})_{int} = \frac{2m\mu}{1-2\nu}\{[2\nu(S_{1111}+S_{1122})+2(1-\nu)S_{3311}]e_{11}^{T}\\
&\quad+[2\nu S_{1133}+(1-\nu)S_{3333}]e_{33}^{T}+(1-2\nu)\varepsilon^{*}\}\\
(\sigma_{33}^{M})_{inh} &= (\sigma_{33}^{I})_{inh} = \frac{2m\mu}{1-2\nu}\{[2\nu(S_{1111}+S_{1122})+2(1-\nu)S_{3311}]e_{11}^{T'}\\
&\quad+[2\nu S_{1133}+(1-\nu)S_{3333}]e_{33}^{T'}+(1+\nu)(1-2\nu)e_{33}^{A}\}
\end{aligned}
\tag{13}
$$

where

$$
\begin{aligned}
e_{33}^{T} &= \frac{m[(1-m)(S_{1111}+S_{1122}+S_{3311})-1]\varepsilon^{*}}{(1-m)^2F(x)-(1-m)G(x)+1}\\
e_{11}^{T} &= e_{22}^{T} = \frac{m[1-(1-m)(2S_{1133}+S_{3333})]\varepsilon^{*}}{2[(1-m)^2F(x)-(1-m)G(x)+1]}\\
e_{33}^{T'} &= \frac{(1-m)[1-(1-m)(2\nu S_{3311}+S_{1111}+S_{1122})]e_{33}^{A}}{(1-m)^2F(x)-(1-m)G(x)+1}\\
e_{11}^{T'} &= e_{22}^{T'} = \frac{(1-m)[(1-m)(\nu S_{3333}+S_{1133})-\nu]e_{33}^{A}}{(1-m)^2F(x)-(1-m)G(x)+1}\\
F(x) &= (S_{1111}+S_{1122})S_{3333}-2S_{1133}S_{3311}\\
G(x) &= S_{1111}+S_{1122}+S_{3333}\\
e_{33}^{A} &= \sigma_{33}^{A}/E
\end{aligned}
\tag{14}
$$

4.2 Inclusion with eigenstrains, $\varepsilon_{11}^{*} = -2\varepsilon_{22}^{*} = -2\varepsilon_{33}^{*} = -\varepsilon^{*}$, under an applied stress, σ_{11}^{A}

The stress components at (a, 0, 0) are expressed by

$$
\begin{aligned}
(\sigma_{11}^{M})_{int} &= (\sigma_{11}^{I})_{int} = \frac{2m\mu}{1-2\nu}\{[(1-\nu)S_{1111}\\
&\quad+\nu(S_{1122}+S_{3311})]e_{11}^{T}\\
&\quad+[(1-\nu)S_{1122}+\nu(S_{1111}+S_{3311})]e_{22}^{T}\\
&\quad+(S_{1133}+\nu S_{3333})e_{33}^{T}+(1-2\nu)\varepsilon^{*}\}
\end{aligned}
$$

$$
\begin{aligned}
(\sigma_{11}^{M})_{inh} &= (\sigma_{11}^{I})_{inh} = \frac{2m\mu}{1-2\nu}\{[(1-\nu)S_{1111}\\
&\quad+\nu(S_{1122}+S_{3311})]e_{11}^{T'}\\
&\quad+[(1-\nu)S_{1122}+\nu(S_{1111}+S_{3311})]e_{22}^{T'}\\
&\quad+(S_{1133}+\nu S_{3333})e_{33}^{T'}\\
&\quad+(1+\nu)(1-2\nu)e_{11}^{A}\}
\end{aligned}
\tag{15}
$$

The stresses at (0, a, 0) are given by

$$
(\sigma_{11}^{M})_{int} = \frac{2\mu}{1-2\nu}\left[\left(\nu(S_{1122}+S_{3311})\right.\right.
$$

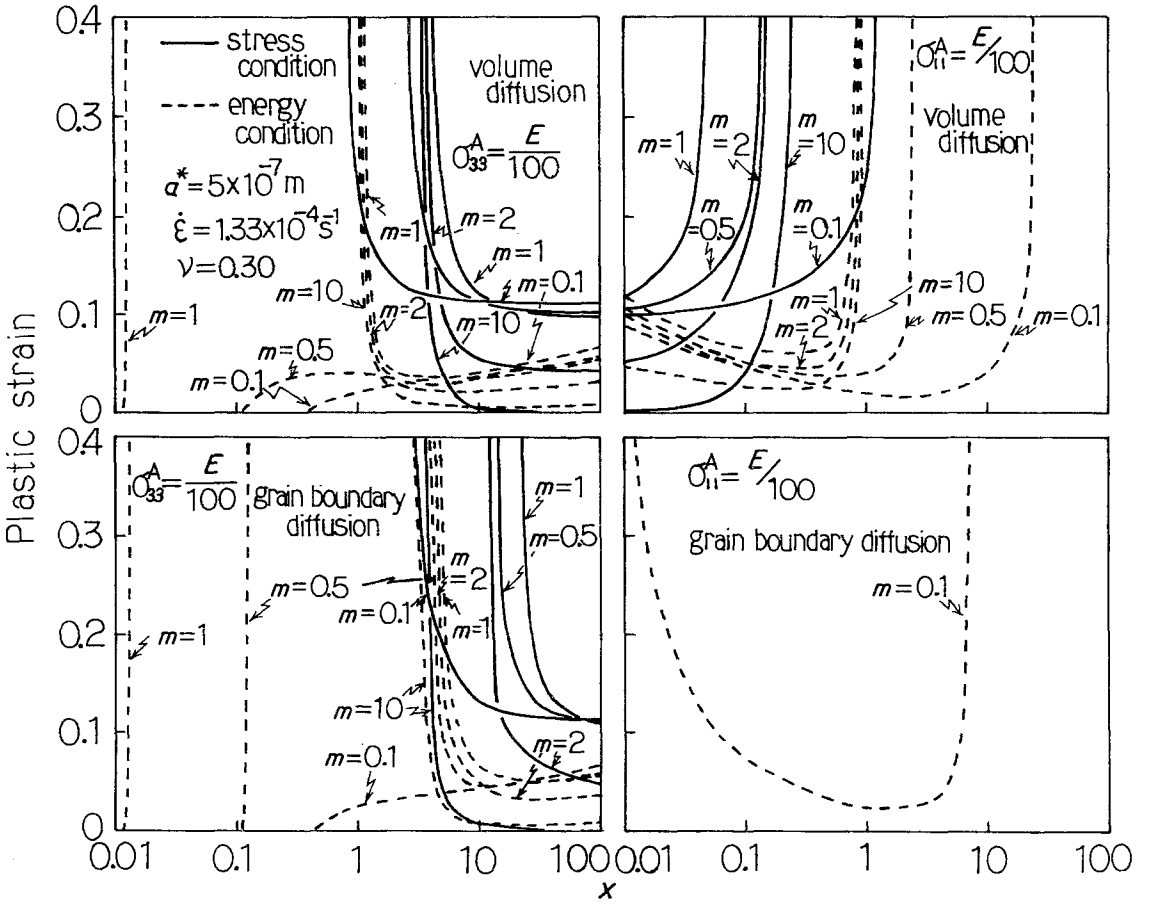

Figure 4 Relation between aspect ratio and the critical strain for fracture initiation at the interface when dynamic recovery by diffusion of atoms is taken into account.

$$
\begin{aligned}
&+ (1-\nu)S_{1111} - \frac{\nu^2}{1-\nu}\Big)e^{T}_{11} \\
&+ [\nu(S_{1111} + S_{3311}) \\
&+ (1-\nu)S_{1122} - \nu]e^{T}_{22} \\
&+ \Big(S_{1133} + \nu S_{3333} - \frac{\nu^2}{1-\nu}\Big)e^{T}_{33}\Big] \\
(\sigma^M_{11})_{inh} &= \frac{2\mu}{1-2\nu}\Big[\Big(\nu(S_{1122} + S_{3311}) \qquad (16)\\
&+ (1-\nu)S_{1111} - \frac{\nu^2}{1-\nu}\Big)e^{T'}_{11} \\
&+ [\nu(S_{1111} + S_{3311}) \\
&+ (1-\nu)S_{1122} - \nu]e^{T'}_{22} \\
&+ \Big(S_{1133} + \nu S_{3333} \\
&- \frac{\nu^2}{1-\nu}\Big)e^{T'}_{33}\Big] + \sigma^A_{11}
\end{aligned}
$$

The stresses at (0, 0, c) are expressed by

$$
\begin{aligned}
(\sigma^M_{11})_{int} &= \frac{2\mu}{1-2\nu}\Big[\Big(\nu(S_{1122} + S_{3311}) \\
&+ (1-\nu)S_{1111} - \frac{\nu^2}{1-\nu}\Big)e^{T}_{11} \\
&+ \Big(\nu(S_{1111} + S_{3311}) \\
&+ (1-\nu)S_{1122} - \frac{\nu^2}{1-\nu}\Big)e^{T}_{22} \\
&+ (S_{1133} + \nu S_{3333} - \nu)e^{T}_{33}\Big] \\
(\sigma^M_{11})_{inh} &= \frac{2\mu}{1-2\nu}\Big[\Big(\nu(S_{1122} + S_{3311}) \qquad (17)\\
&+ (1-\nu)S_{1111} - \frac{\nu^2}{1-\nu}\Big)e^{T'}_{11} \\
&+ \Big(\nu(S_{1111} + S_{3311}) \\
&+ (1-\nu)S_{1122} - \frac{\nu^2}{1-\nu}\Big)e^{T'}_{22} \\
&+ (S_{1133} + \nu S_{3333} - \nu)e^{T'}_{33}\Big] + \sigma^A_{11}
\end{aligned}
$$

where

$$
\begin{aligned}
e_{11}^{T} &= \frac{m[(1-m)^2H(x) + (1-m)I(x) - 2]\varepsilon^*}{2[(1-m)U(x)+1][(1-m)^2F(x) - (1-m)G(x)+1]} \\
e_{22}^{T} &= \frac{m[(1-m)^2J(x) - (1-m)L(x)+1]\varepsilon^*}{2[(1-m)U(x)+1][(1-m)^2F(x) - (1-m)G(x)+1]} \\
e_{33}^{T} &= \frac{m[1-(1-m)T(x)]\varepsilon^*}{2[(1-m)^2F(x) - (1-m)G(x)+1]} \\
e_{11}^{T'} &= \frac{(m-1)[(1-m)^2V(x) + (1-m)W(x) - 1]e_{11}^{A}}{[(1-m)U(x)+1][(1-m)^2F(x) - (1-m)G(x)+1]} \\
e_{22}^{T'} &= \frac{(m-1)[(1-m)^2X(x) - (1-m)Y(x) + v]e_{11}^{A}}{[(1-m)U(x)+1][(1-m)^2F(x) - (1-m)G(x)+1]} \\
e_{33}^{T'} &= \frac{(m-1)[v-(1-m)Z(x)]e_{11}^{A}}{(1-m)^2F(x) - (1-m)G(x)+1} \\
H(x) &= S_{1133}(3S_{3311} + S_{1122} - S_{1111}) - S_{3333}(2S_{1111} + S_{1122}) \\
I(x) &= 2S_{1111} + 2S_{3333} + S_{1122} + S_{1133} \\
J(x) &= S_{3333}(2S_{1122} + S_{1111}) - S_{1133}(3S_{3311} + S_{1111} - S_{1122}) \\
L(x) &= 2S_{1122} + S_{1111} + S_{3333} - S_{1133} \\
T(x) &= S_{1111} + S_{1122} + S_{3311} \\
U(x) &= S_{1122} - S_{1111} \\
V(x) &= S_{1133}S_{3311} - S_{3333}S_{1111} + v[S_{1133}(S_{3311} + S_{1122} - S_{1111}) - S_{3333}S_{1122}] \\
W(x) &= S_{1111} + S_{3333} + v(S_{1122} + S_{1133}) \\
X(x) &= S_{3333}S_{1122} - S_{1133}S_{3311} + v[S_{3333}S_{1111} - S_{1133}(S_{3311} + S_{1111} - S_{1122})] \\
Y(x) &= S_{1122} + v(S_{1111} + S_{3333} - S_{1133}) \\
Z(x) &= S_{3311} + v(S_{1111} + S_{1122} - S_{3311}) \\
e_{11}^{A} &= \sigma_{11}^{A}/E
\end{aligned}
\tag{18}
$$

The Eshelby tensor, S_{ijkl}, is given elsewhere [3, 11, 12]. Fig. 6 shows the stress components at the interface of an inclusion calculated by the above equations. Those values are normalized by an external stress (σ_{33}^{A} or σ_{11}^{A}) or $E\varepsilon^*$ in this figure. The stress values of $(\sigma_{33}^{M})_{int}$ and $(\sigma_{33}^{M})_{inh}$ at polar point B ((0, 0, c)) are greater than those at equator points A ((a, 0, 0)) and C ((0, a, 0)) at large values of the aspect ratio (x) when σ_{33}^{A} is an external stress. Fracture initiation can occur at polar point B in this case. Both $(\sigma_{11}^{M})_{int}$ and $(\sigma_{11}^{M})_{inh}$ have maximum values at A for small values of x when σ_{11}^{A} is applied. Therefore, decohesion at the interface of an inclusion can be initiated at this point of an inclusion of small aspect ratio. Shibata and Ono [4] considered that decohesion at the interface of an inclusion of small aspect ratio (x) occurs at point A (or C) due to the plastic deformation effect ($(\sigma_{33}^{M})_{int}$) with eigenstrains, $\varepsilon_{33}^* = -2\varepsilon_{11}^* = -2\varepsilon_{22}^* = -\varepsilon^*$, under an external stress, σ_{33}^{A}. But this is improbable because $(\sigma_{33}^{M})_{int}$ is negative at that point in this case. Their result clearly conflicts with the experimental observation of steels with oblate MnS inclusions deformed at room temperature [13]. As is known from Figs. 4 and 5, even at high temperatures the decrease in stress concentration due to recovery by diffusion of atoms is smaller at larger aspect ratio when the eigenstrains are $\varepsilon_{33}^* = -2\varepsilon_{11}^* = -2\varepsilon_{22}^* = -\varepsilon^*$, while it is larger at larger aspect ratio when $\varepsilon_{11}^* = -2\varepsilon_{22}^* = -2\varepsilon_{33}^* = -\varepsilon^*$. The effect of recovery on stress concentration is smaller for larger particle size. It was suggested

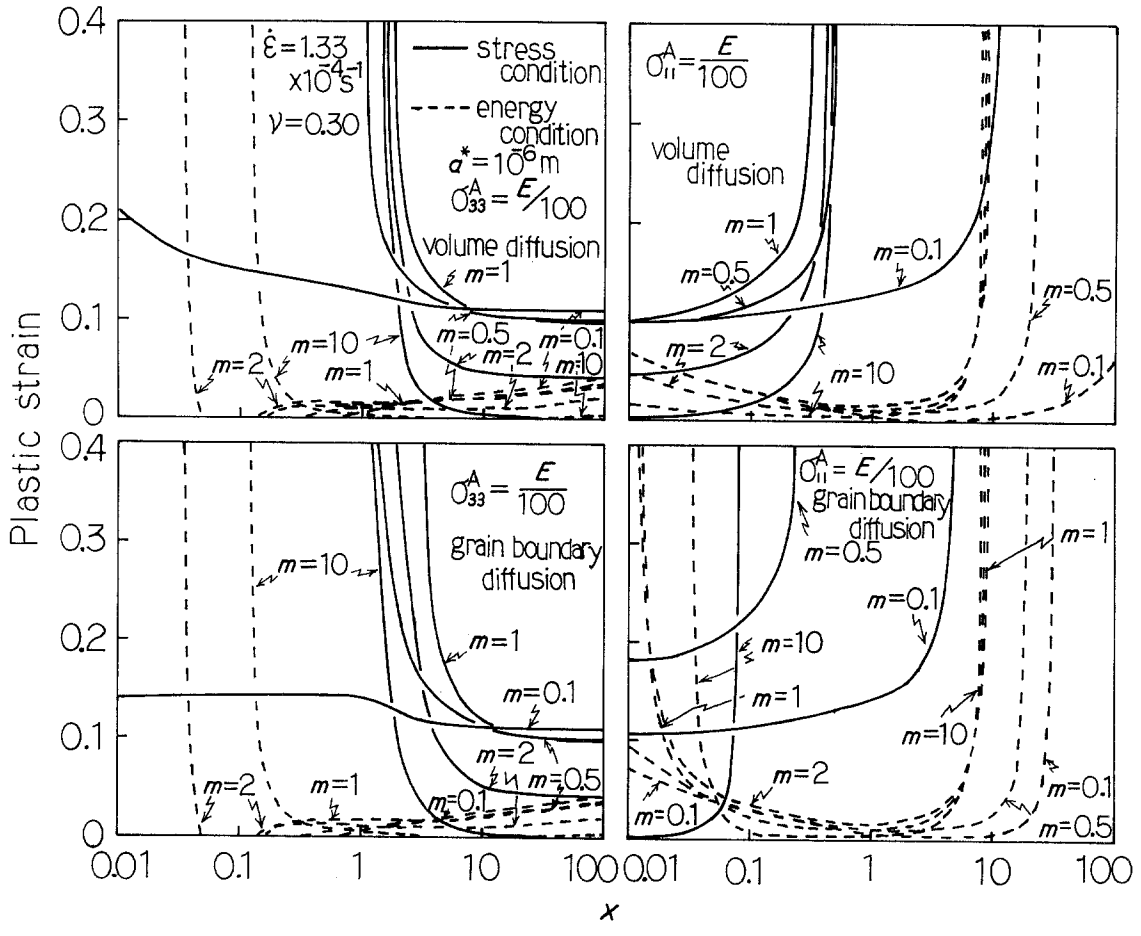

Figure 5 Effect of particle size on the critical strain for fracture initiation at the interface when dynamic recovery by diffusion of atoms is taken into account.

that void formation at the interface of an inclusion clearly depends on its shape and size also in the high-temperature deformation of a cobalt-base superalloy [14].

5. Fracture initiation of fibre-reinforced composite materials

Decohesion at the second phase–matrix interface or fracture in the matrix can be caused by internal stresses induced by transformation of the second phase or by differences in thermal expansion between the second phase and the matrix upon cooling from high temperatures [7]. The equivalent inclusion method is also applicable to the understanding of fracture initiation of composite materials containing a large amount of high-strength fibres ($x = c/a \gg 1$, $V = \frac{4}{3}\pi a^2 c$) when the eignstrains $\varepsilon^*_{11} = \varepsilon^*_{22} = pe^*$ and $\varepsilon^*_{33} = re^*$ occur only in the fibres. If the interaction among the fibres and the image force term are taken into account [15], the internal stresses and the elastic strain energy, E_{el}, are given by

$$\sigma^I_{11} = \sigma^I_{22} = -\frac{2m(p + rv^*)\mu e^*}{1 - 2v^* + m}(1 - f)$$

$$\sigma^I_{33} = -\frac{2m\{2pv^* + r[m(1 + v^*) + 1 - v^*]\}\mu e^*}{1 - 2v^* + m}(1 - f) \tag{19}$$

$$E_{el} = \frac{Nm\mu e^{*2}V}{1 - 2v^* + m}\{2p^2 + 4v^*rp + r^2[m(1 + v^*) + 1 - v^*]\}(1 - f)$$

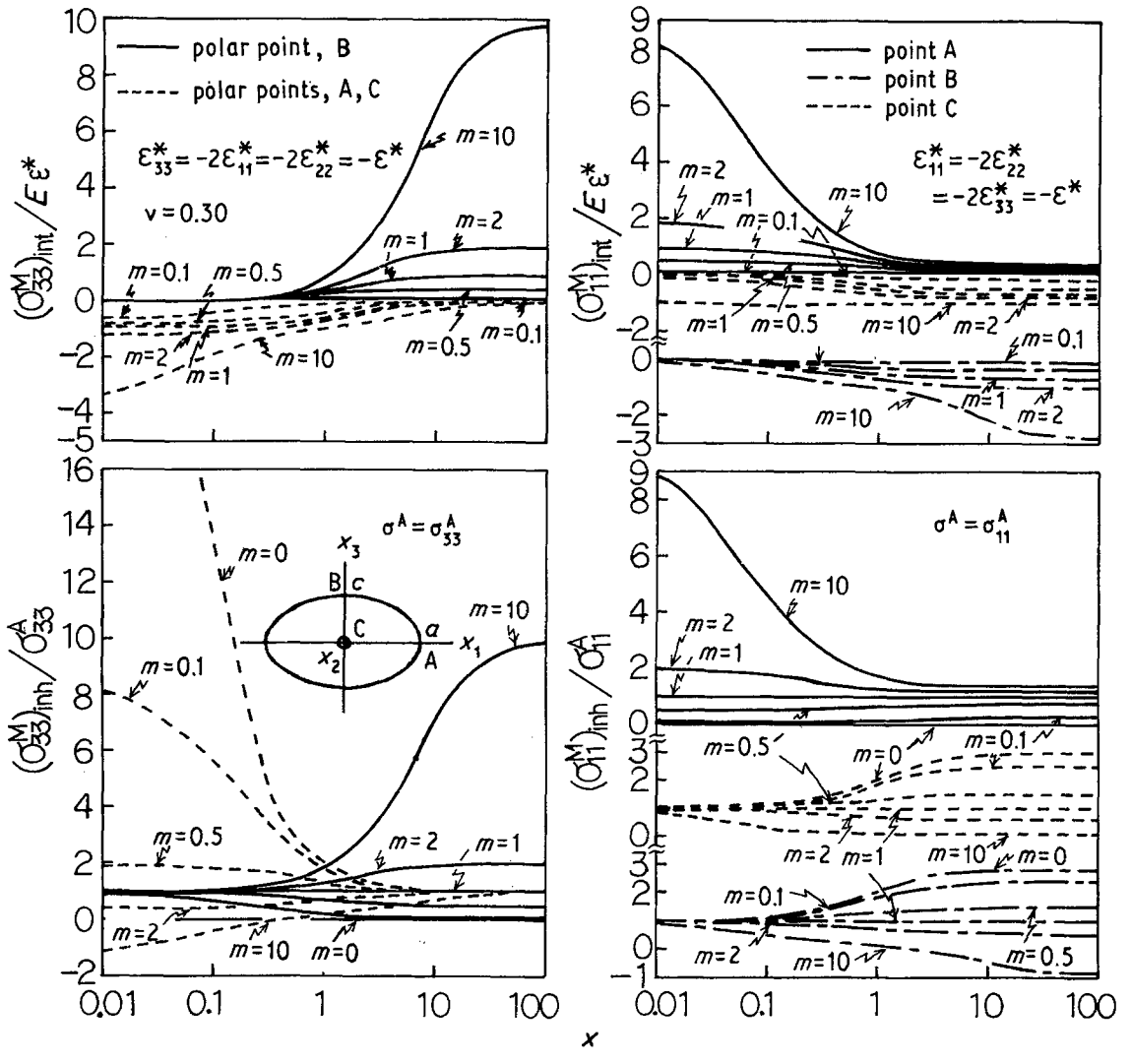

Figure 6 The stress components at the interface of an inclusion.

where N is the number of fibres. The stresses just outside a fibre in (R, θ, z) coordinates (z-axis parallel to x_3-axis) are obtained by the elastic solution of a cylinder under internal pressure and axial stress [16], provided that the fibre is extremely long. The stress components in the middle portion of a fibre are given by

$$
\begin{aligned}
(\sigma_\theta)_{R=a} &= \frac{2m(p + rv^*)\mu e^*}{1 - 2v^* + m}(1 + f) \\
(\sigma_R)_{R=a} &= -\frac{2m(p + rv^*)\mu e^*}{1 - 2v^* + m}(1 - f) \qquad (20) \\
\sigma_z &= \frac{2m\{2pv^* + r[m(1 + v^*) + 1 - v^*]\}\mu e^*}{1 - 2v^* + m} f
\end{aligned}
$$

where σ_z is independent of R. The absolute values of σ_θ and σ_R have maxima at $R = a$. Decohesion at the interface of the fibre can occur when $e^* < 0$, while fracture of the matrix is expected when $e^* > 0$.

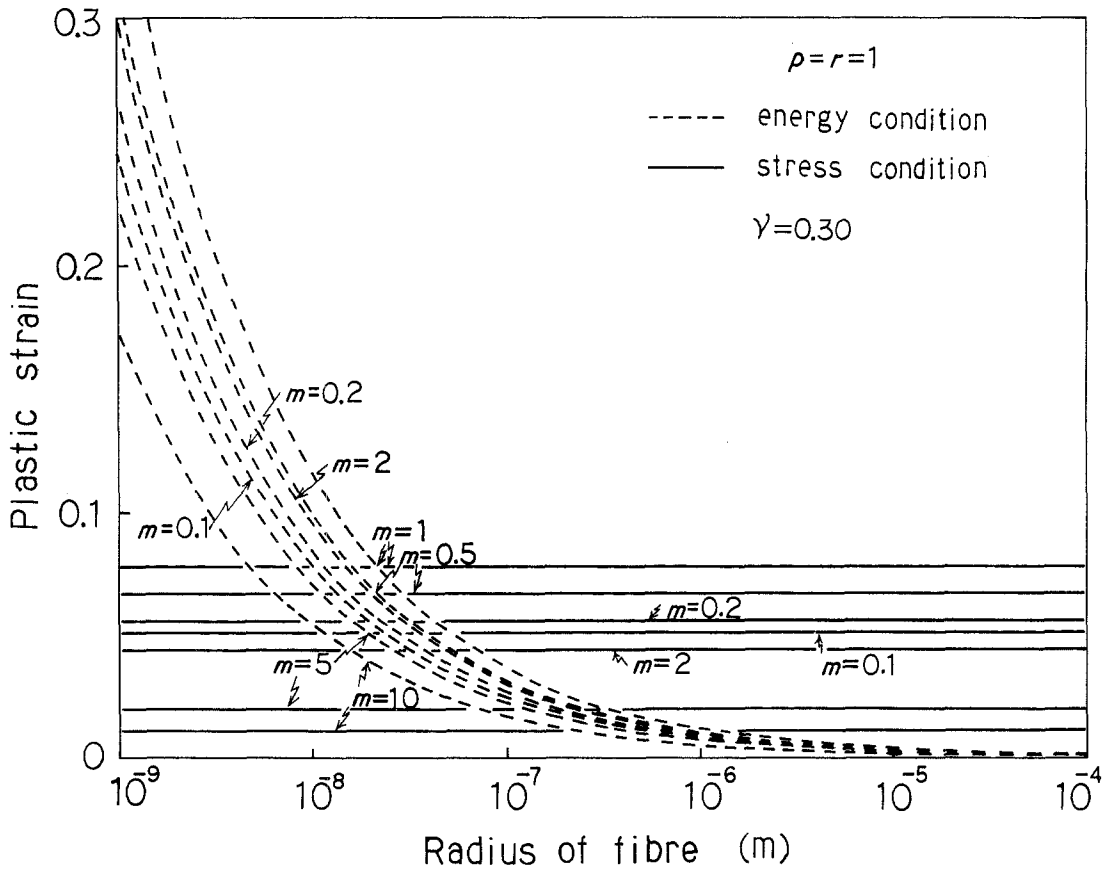

Figure 7 Relation between fibre radius and the critical strain for fracture initiation at the interface of a fibre with isotropic eigenstrain.

5.1. Decohesion at the interface of the fibre ($e^* < 0$)

It is considered here that the stress condition for decohesion at the interface of the fibre is satisfied when the internal tensile stress exceeds $E^*/10$ or $E/10$. As for the energy condition, it is assumed that the condition is fulfilled when the elastic strain energy becomes greater than the increase of surface energy due to decohesion, namely

$$E_{el}/N - S(\gamma_I + \gamma_M - \gamma_{I-M}) > 0 \quad (21)$$

where $S = \pi^2 ac$. For isotropic eigenstrain ($p = r = 1$), decohesion is caused by the axial internal stress σ^I_{33} of a fibre, because $\sigma^I_{33} > \sigma^I_{11}$ (or σ^I_{22}) when $m > 0$.

Fig. 7 shows the values of the critical strains for both conditions calculated from the above equations plotted against the radius of the fibre for $v^* = v = 0.30$ and $f = 0.10$. Both critical strains have maximum values when $m = 1$. For uniaxial eigenstrain ($p = 0$, $r = 1$), the magnitude of σ^I_{33} is also important. In contrast, the stress condition is defined by σ^I_{11} ($= \sigma^I_{22}$) for biaxial eigenstrain ($p = 1$, $r = 0$), since σ^I_{11} ($= \sigma^I_{22}$) $> \sigma^I_{33}$. Fig. 8 shows the value of the critical strains for $v^* = v = 0.30$ and $f = 0.10$ plotted against fibre radius. The value of m has little effect on the critical strains for $p = 0$ and $r = 1$ when $m < 1$ and for $p = 1$ and $r = 0$ when $m > 1$.

5.2. Fracture initiation in the matrix ($e^* > 0$)

The fracture of brittle matrix can be induced by thermal stress or transformation of the second phase. Fracture of the matrix normal to the θ-direction (in z–θ plane) occurs only when $p = 1$ and $r = 0$, because $(\sigma_\theta)_{R=a}$ is always greater than σ_z (Equation 20). In contrast, fracture of the matrix is expected to occur vertically to the fibre axis when $\sigma_z > (\sigma_\theta)_{R=a}$. This type of fracture can occur for $p = 0$ and $r = 1$ if

$$m > \frac{v^* - f(1 - 2v^*)}{(1 + v^*)f} \quad (22)$$

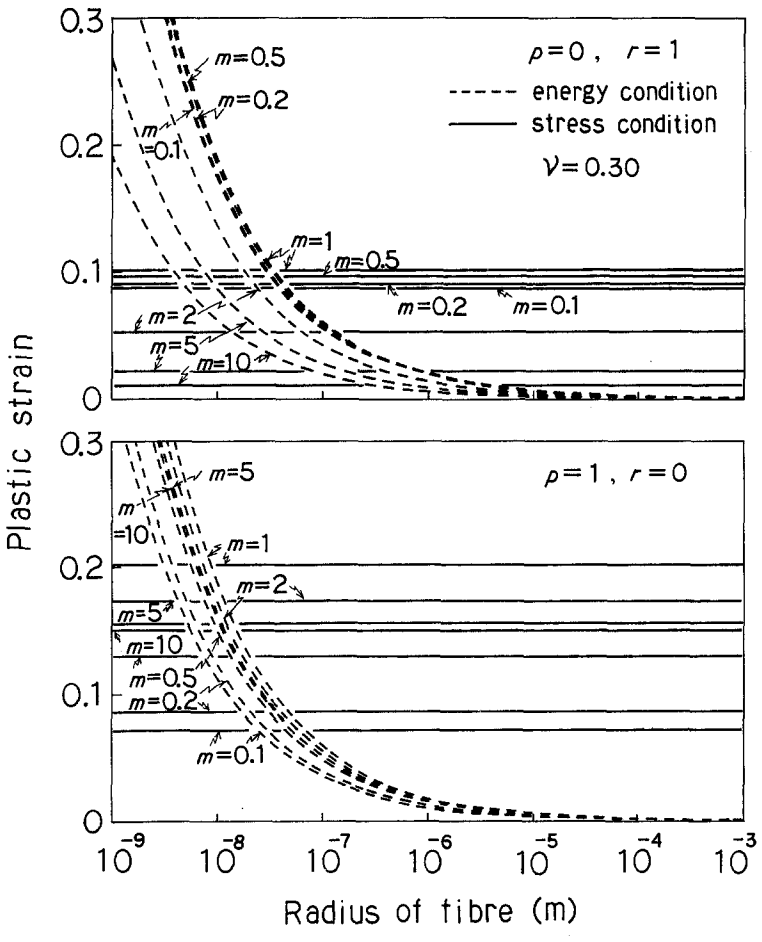

Figure 8 Relation between fibre radius and the critical strain for fracture initiation with anisotropic eigenstrain.

Fracture can also occur for isotropic eigenstrain ($p = r = 1$) if

$$m > \frac{1}{f} \geqslant 1 \tag{23}$$

The axial stress in the matrix of the material is very large for isotropic eigenstrain when the rigidity of the second phase is much higher than that of the matrix (large m). For example, in concrete structures strengthened with steel bars ($m \simeq 10$), fracture of the concrete matrix with low tensile strength (usually lower than $5 \times 10^{-5} E$) can occur to the large axial stress induced by a slight volume increase of steel bars as a result of oxidation or by the constriction of the concrete matrix during drying [17]. The axial internal stress in the matrix, σ_z, increases with increase of the volume fraction of steel bars (Equation 20). Therefore, care should be taken in the material design of concrete structures as well as in the protection of steel bars from severe oxidation.

6. Conclusion

Fracture initiation at an inclusion in a metallic material both at room and high temperatures has been discussed theoretically using the equivalent inclusion method and the results of analysis of a previous study.

It was shown that the critical strain for fracture initiation at the inclusion–matrix interface is strongly affected by shape, size, orientation and rigidity of the inclusion, and by the presence of external stress. Dynamic recovery by the diffusion of atoms, which is also dependent on several factors including size, shape and orientation of the inclusion, and so on, has a noticeable effect on decohesion at the interface of the inclusion in the high temperature range.

Fracture initiation of a brittle material strengthened with strong fibres was also predicted using the equivalent inclusion method when isotropic or anisoptropic eigenstrain occurs only in the fibres.

Appendix

The values of A_1, B_1 and $\bar{D}_1$ before fracture initiation can be calculated using the Eshelby tensor, S_{ijkl} [1–3, 7, 11, 12]

A.1. Inclusion with eigenstrains, $\varepsilon^*_{33} = -2\varepsilon^*_{11} = -2\varepsilon^*_{22} = -\varepsilon^*$, under an applied stress, σ^{A}_{33}

$$
\begin{aligned}
A_1 &= -2m\left((S_{1111}+S_{1122}-2S_{3311})\frac{e^{\mathrm{T}}_{11}}{\varepsilon^*}+(S_{1133}-S_{3333})\frac{e^{\mathrm{T}}_{33}}{\varepsilon^*}-\frac{3}{2}\right)\\
B_1 &= -\frac{m[(1-m)(S_{1111}+S_{1122}+S_{3311})-1]}{(1-m)^2F(x)-(1-m)G(x)+1}\\
\bar{D}_1 &= -\frac{(1-m)[1-(1-m)(2\nu S_{3311}+S_{1111}+S_{1122})]}{2(1+\nu)[(1-m)^2F(x)-(1-m)G(x)+1]}
\end{aligned}
\tag{A.1}
$$

where

$$
\begin{aligned}
e^{\mathrm{T}}_{33} &= -mF_{\mathrm{d}}(x)\varepsilon^*/F_{\mathrm{ab}}(x)\\
e^{\mathrm{T}}_{11} &= e^{\mathrm{T}}_{22} = mF_{\mathrm{b}}(x)\varepsilon^*/[2F_{\mathrm{ab}}(x)]\\
F_{\mathrm{ab}}(x) &= (1-m)F_{\mathrm{a}}(x)+F_{\mathrm{b}}(x)\\
F_{\mathrm{a}}(x) &= (1-\nu)[(S_{1111}+S_{1122})(1-S_{3333})+2S_{3311}S_{1133}]-2\nu S_{1133}
\end{aligned}
$$

A.2. Inclusion with eigenstrains, $\varepsilon^*_{11} = -2\varepsilon^*_{22} = -2\varepsilon^*_{33} = -\varepsilon^*$, under an applied stress, σ^{A}_{11}

$$
\begin{aligned}
A_1 &= -m\left((S_{1122}+S_{3311}-2S_{1111})\frac{e^{\mathrm{T}}_{11}}{\varepsilon^*}+(S_{3311}+S_{1111}-2S_{1122})\frac{e^{\mathrm{T}}_{22}}{\varepsilon^*}\right.\\
&\quad\left.+(S_{3333}-S_{1133})\frac{e^{\mathrm{T}}_{33}}{\varepsilon^*}-3\right)\\
B_1 &= -\frac{m[(1-m)^2H(x)+(1-m)I(x)-2]}{2[(1-m)U(x)+1][(1-m)^2F(x)-(1-m)G(x)+1]}\\
\bar{D}_1 &= -\frac{(m-1)[(1-m)^2V(x)+(1-m)W(x)-1]}{2(1+\nu)[(1-m)U(x)+1][(1-m)^2F(x)-(1-m)G(x)+1]}
\end{aligned}
\tag{A.2}
$$

A_2, B_2 and $\bar{D}_2$ immediately after fracture initiation are also expressed by the Eshelby tensor [1–3, 7, 11, 12].

A.3. Inclusion with eigenstrains, $\varepsilon^*_{33} = -2\varepsilon^*_{11} = -2\varepsilon^*_{22} = -\varepsilon^*$, under an applied stress, σ^{A}_{33}

$$
\begin{aligned}
A_2 &= -\frac{2m(1+\nu)}{1-\nu}\\
&\quad\times\left((S_{1111}+S_{1122})\frac{e^{\mathrm{T}}_{11}}{\varepsilon^*}+S_{1133}\frac{e^{\mathrm{T}}_{33}}{\varepsilon^*}-\frac{1}{2}\right)\\
B_2 &= \frac{mF_{\mathrm{d}}(x)}{F_{\mathrm{ab}}(x)}\\
\bar{D}_2 &= -\frac{1}{2(1+\nu)F_{\mathrm{ab}}(x)}\\
&\quad\times[(1-m)F_{\mathrm{c}}(x)-(1+\nu)(1-2\nu)]
\end{aligned}
\tag{A.3}
$$

$$
\begin{aligned}
F_{\mathrm{b}}(x) &= (1-\nu)(S_{3333}-1)+2\nu S_{1133}\\
F_{\mathrm{c}}(x) &= (1-\nu)(S_{1111}+S_{1122}+2\nu S_{3311})-2\nu^2\\
F_{\mathrm{d}}(x) &= \nu(S_{1111}+S_{1122}-1)+(1-\nu)S_{3311}
\end{aligned}
$$

A.4. Inclusion with eigenstrains, $\varepsilon^*_{11} = -2\varepsilon^*_{22} = -2\varepsilon^*_{33} = -\varepsilon^*$, under an applied stress, σ^{A}_{11}

$$
\begin{aligned}
A_2 &= -\frac{m(1+\nu)}{1-\nu}\left((S_{1122}+S_{3311})\frac{e^{\mathrm{T}}_{11}}{\varepsilon^*}\right.\\
&\quad+(S_{1111}+S_{3311})\frac{e^{\mathrm{T}}_{22}}{\varepsilon^*}\\
&\quad\left.+(S_{1133}+S_{3333})\frac{e^{\mathrm{T}}_{33}}{\varepsilon^*}-1\right)\\
B_2 &= -m[(1-m)Q_2(x)-R_2(x)]/[2F_{\mathrm{f}}(x)]
\end{aligned}
\tag{A.4}
$$

$$\bar{D}_2 = -[(1-m)^2 J_2(x) + (1-m)K_2(x) - (1-2\nu)(1+\nu)]/[2(1+\nu)F_f(x)]$$

where

$$e^T_{11} = m[(1-m)Q_2(x) - R_2(x)]\varepsilon^*/[2F_f(x)]$$

$$e^T_{22} = -m[(1-m)S_2(x) - H_2(x)]\varepsilon^*/[2F_f(x)]$$

$$e^T_{33} = -m[(1-m)U_2(x) - H_2(x)]\varepsilon^*/[2F_f(x)]$$

$$F_f(x) = (1-m)^2 F_2(x) + (1-m)G_2(x) + H_2(x)$$

$$F_2(x) = S_{3311}\{(S_{1111} - S_{1122}) \times [\nu - 2(1-\nu)S_{1133}] + (1-2\nu)S_{1133}\} + S_{3333}\{(1-\nu)S_{1111}(S_{1111} - 1) + S_{1122}[\nu - (1-\nu)S_{1122}]\}$$

$$G_2(x) = (S_{1122} - S_{1111}) \times [(1-\nu)(S_{1122} + S_{1111}) + \nu S_{3311}] - S_{3333}[\nu S_{1122} + (1-\nu)(S_{1111} - 1)] + (1-\nu)S_{1111} - \nu S_{1122} + S_{3311}(S_{1133} - \nu)$$

$$H_2(x) = (1-\nu)(S_{1111} - 1) + \nu(S_{1122} + S_{3311})$$

$$J_2(x) = S_{1133}[(1+\nu)(1-\nu)S_{3311} - \nu(1-\nu)(S_{1111} - S_{1122}) - \nu^2] - S_{3333}[(1-\nu)S_{1111} + \nu(1-\nu)S_{1122} - \nu^2] - \nu^2(S_{3311} - S_{1111})$$

$$K_2(x) = (1 - \nu - \nu^2)(S_{1111} + S_{3333}) + \nu(1-\nu)S_{1122} + \nu^2(S_{3311} - 2) + \nu S_{1133}$$

$$Q_2(x) = S_{1133}[(1-\nu)(S_{1111} - S_{1122}) - (1+\nu)S_{3311} + \nu] + S_{3333}[2\nu S_{1111} + (1-\nu)S_{1122} - \nu] + \nu(S_{3311} - S_{1111})$$

$$R_2(x) = \nu(S_{1111} + S_{3311} + S_{3333} - 2) + (1-\nu)S_{1122} + S_{1133}$$

$$S_2(x) = S_{1133}[(1-\nu)(S_{1122} - S_{1111}) - (1+\nu)S_{3311} + 1 - \nu] + S_{3333}[2\nu S_{1122} + (1-\nu)(S_{1111} - 1)] + \nu(S_{3311} - S_{1122})$$

$$U_2(x) = (S_{1111} - S_{1122}) \times [(1-\nu)(S_{1111} + S_{1122}) - (1-3\nu)S_{3311}] - (1-\nu)S_{1111} + \nu S_{1122} + (1-2\nu)S_{3311}$$

References

1. K. TANAKA, T. MORI and T. NAKAMURA, *Phil. Mag.* **21** (1970) 267.
2. *Idem, Trans. Iron Steel Inst. Japan* **11** (1971) 383.
3. J. D. ESHELBY, *Proc. R. Soc. A* **241** (1957) 376.
4. M. SHIBATA and K. ONO, *Acta Metall.* **26** (1978) 921.
5. R. HORIUCHI and M. OTSUKA, *Bull. Japan Inst. Met.* **22** (1983) 293.
6. M. TANAKA and H. IIZUKA, *J. Mater. Sci.* **19** (1984) 3976.
7. W. DONALD and P. W. McMILLAN, *ibid.* **11** (1976) 949.
8. W. BEERE and M. V. SPEIGHT, *Met. Sci.* **12** (1978) 593.
9. M. A. SADOWSKY and E. STERNBERG, *J. Appl. Mech.* **14** (1947) 191.
10. Z. A. MOSCHOVIDIS and T. MURA, *ibid.* **42** (1975) 847.
11. T. MURA, "Micromechanics of Defects in Solids" (Martinus Nijhoff, The Hague, 1982) p. 63.
12. T. MURA and T. MORI, "Micromechanics" (Baifukan, Tokyo, 1976) p. 23.
13. W. ROBERTS, B. LEHTINEN and K. E. EASTERLING, *Acta Metall.* **24** (1976) 745.
14. J. P. HAMMOND, "Ductility and Toughness Considerations in Elevated Temperature Service" (MPC-8), edited by G. V. Smith (ASME, New York, 1978) p. 63.
15. T. MORI and K. TANAKA, *Acta Metall.* **21** (1973) 571.
16. R. HILL, "The Mathematical Theory of Plasticity" (Clarendon Press, Oxford, 1960) p. 106.
17. "Guide and Commentary on Prevention of Salt Attack in Road Bridges", edited by Japan Road Association (Maruzen, Tokyo, 1984) p. 1.

Received 28 September
and accepted 3 December 1984